# Implementation of a Synthetic Turbulence Generator for RANS/LES Interface in TAU-Code

Daniela Gisele François* and Rolf Radespiel,†
*Institute of Fluid Mechanics,38108, Braunschweig, Germany*

**Abstract**

**This work describes the status of an implementation in progress which aims to include into the DLR TAU-Code a flexible synthetic turbulence generator. The synthetic turbulence generator will be used to provide a physically realistic velocity fluctuation field for embedded LES approaches. The features of the selected algorithm are tested on a 2D flat plate boundary layer. Results show that the turbulence generator can accurately reconstruct the anisotropic Reynolds stress tensors of the inhomogeneous boundary layer taken as reference. In addition, the model has been shown to contain information of time and special correlation. Further tests are required to be performed in 3D study cases so as to evaluate the effectiveness of the model to speed up the transition into realistic resolved turbulence in DES approaches.**

# Nomenclature

| | |
|---|---|
| $\delta$ | Boundary layer thickness $[m]$ |
| $\delta_0$ | Boundary layer thickness at the RANS-LES interface $[m]$ |
| $\Delta x, \Delta y, \Delta z$ | Grid spacing $[m]$ |
| $\Delta t$ | Time Step $[s]$ |
| $E$ | Non-dimensional spectral energy[-] |
| $\epsilon$ | Dissipation rate $[\frac{m^2}{s^3}]$ |
| $\epsilon^h$ | Homogeneous part of $\epsilon$ $[\frac{m^2}{s^3}]$ |
| $f_d$ | Blending function [-] |
| $k$ | Wave number $[\frac{1}{m}]$ |
| $k_e$ | Wave number of the most energetic eddies $[\frac{1}{m}]$ |
| $k_t$ | Turbulence kinetic energy $[\frac{m^2}{s^2}]$ |
| $r$ | Position vector $[m]$ |
| $Re$ | Reynolds number [-] |
| $\rho$ | Density $[\frac{kg}{m^3}]$ |
| $t$ | Time $[s]$ |
| $\tau$ | Time Scale $[s]$ |

*Research scientist
†Professor

| | |
|---|---|
| $\overline{u_i' u_j'}$ | Reynolds stress tensor $[\frac{m^2}{s^2}]$ |
| $u, v, w$ | Components of the flow velocity field $[\frac{m}{s}]$ |
| $U, V, W$ | Components of the mean flow velocity field $[\frac{m}{s}]$ |
| $u', v', w'$ | Components of the fluctuation velocity field $[\frac{m}{s}]$ |
| $U', V', W'$ | Components of the time-correlated fluctuation velocity field $[\frac{m}{s}]$ |
| $x, y, z$ | Components of the position vector $[m]$ |
| $()^+$ | Dimensionless distance [-] |

# 1 Introduction

Performing reliable simulations of massively separated flow on airfoils, wings and nacelles is one of the most important challenges in the aeronautical industry of today.
The availability of trustworthy numerical solutions would allow a better understanding of flow processes taking part during critical flight phases, and leads to the optimization of design processes while enhancing flight safety and increasing operational ranges.
DNS (Direct Numerical Simulation) and LES (Large Eddy Simulation) would be proper approaches in order to provide this information. But their excessive computational cost makes them unsuitable or even unachievable for industrial purposes. Therefore, DES (Detached Eddy Simulation) approaches arise as promising model to accomplish this aim.
These strategies attempt to take advantage of the good capabilities of the RANS model to solve attached boundary layer at low computational cost and the good capabilities of the LES model to precisely describe complex turbulent detached flows.
Several approaches were developed for DES application (DDES [1] [2], IDDES[3] [2] and ADDES [4]). DDES and IDDES have failed in the detection of the separation onset giving rise to a delay in the RANS/LES mode switching and therefore, the turbulence is not resolved in that area. For the sake of correcting that behaviour, ADDES introduces algebraic sensors which evaluate the boundary layer properties in order to detect the boundary layer thickness and the separation onset.
Works have already been performed at the Institute of Fluid Mechanics of TU Braunschweig in this direction. The last implementation was the $\epsilon^h$-ADDES [4] which is already incorporated into the internal development version of the TAU-Code. This model uses the $\epsilon^h$-RSM [5] as RANS background model. Using $\epsilon^h$-RSM [6] provides a more accurate solution of the boundary layer development rather than other classical models like SA (Spalart-Allmaras [7]) and improves considerably the detection of pressure-induced separation. Important drawbacks of previous DES versions are overcome by this last one. These are the underestimation of the boundary layer thickness which may lead to spurious modelled stress depletion and the lack of detecting pressure-induced separation.
But the major shortcoming of the hybrid approaches still remains. In hybrid RANS/LES simulations, the RANS solution immediately before the interface transfers only mean values into the LES domain which are interpreted by LES model as instantaneous values and consequently all the turbulence information is missing during this process (RANS to LES transition). This leads to a long transition distance until the LES model resolves the turbulence content of the flow.
In order to shorten this transition distance, there are several Ad Hoc methods assigned to artificially provide the inlet of LES domain with the unsteadiness of the flow missed during the transition. There are three main approaches in order to generate these fluctuations. These are

using external data base from DNS or fully LES solutions, recycling procedures and synthetic turbulence generators [8] [9]. Each of them has their own advantages and disadvantages. External data bases are very accurate, but they generally require extra expensive computations and extensive storage load and they lack flexibility. Recycling procedures are very cheap and they achieve short adaptation distances but they induce spurious frequencies. Finally, synthetic turbulence generators are flexible (applicable to complex geometries), they require only mean velocity and Reynolds stresses which are provided by RANS solutions during run time. They use low order statistics and do not generate spurious frequencies. But, on the other hand, they are known to produce a longer adaptation distance. The aim of the present work is to reduce considerably the extended transition area of $\epsilon^h$-ADDES implementation by including a flexible synthetic turbulence generator into the TAU-Code. And thus have at disposal an $\epsilon^h$-ADDES implementation able to provide reliable solutions of massively separated flows when detailed information of the turbulence is required.

# 2 Numerical method

The selected synthetic turbulence generator is based on the work of D. Adamian and A. Travin [10] which is an improved version of the Batten approach [11] for inhomogeneous turbulence with anisotropic Reynolds stress tensor.
This model is based on the concept that turbulence can be defined as a superposition of coherent structures. The fluctuating velocity field is defined as a superposition of Fourier modes whilst the amplitude of each mode is determined following a spectral approach.
Consequently, the fluctuating velocity field generated by this method provides the same Reynolds stresses distributions as the RANS model upstream of the transition and it has a defined spectral distribution which is based on statistical parameters also supplied by the RANS model. These include the turbulence kinetic energy ($k_t$), dissipation rate ($\epsilon$), mean bulk velocity of the flow and some geometrical considerations (grid spacing & distance to the wall). The reason for the selection of this method was based on its completeness in the physical description and because authors report rapid transition to fully developed turbulence [10]. The velocity fluctuation is defined as:

$$u'(\mathbf{r},t) = f_d A\sqrt{6}\sum_{n=1}^{N}\sqrt{q^n}\sigma^{\mathbf{n}} cos(k^n \mathbf{d^n}\mathbf{r} + \Phi^n + S^n\frac{t}{\tau}) \tag{1}$$

where $f_d$ is a blending function that needs to be adjusted by means of tests so as to ensure a smooth transition of the resolved flow properties through the RANS-LES interface as well as the correct order of magnitude of the resolved turbulence. $A$ is the lower triangular matrix obtained from the Cholesky decomposition of the Reynolds stress tensor which ensures that the synthetic turbulence generator produces the same Reynolds stress distribution as the RANS solution upstream of the transition. $q^n$ is the normalized amplitude of each mode and it is obtained from the modelled spectral distribution as defined by eq. 2 . $\sigma^{\mathbf{n}}$ and $\mathbf{d^n}$ are random vectors whilst $\phi^n$ and $S^n$ are random values. Each of them satisfies certain distribution constraints.

$$q^n = \frac{E(k^n)\Delta k^n}{\sum_{n=1}^{N} E(k^n)\Delta k^n} \tag{2}$$

therefore, $q^n$ satisfies the condition:

$$\sum_{n=1}^{N} q^n = 1 \tag{3}$$

$E(k_n)$ is obtained from a modified non-dimensional von Karman spectrum.

$$E(k^n) = \frac{(\frac{k}{k_e})^4}{[1 + 2.4(\frac{k}{k_e})^2]^{17/6}} f_\eta f_{cut} \tag{4}$$

In eq. 4, $f_\eta$ and $f_{cut}$ are damping functions that damp the spectrum for wave numbers larger than the Kolmogorov length scale and for the Nyquist wave number respectively (fig. 1 ). In

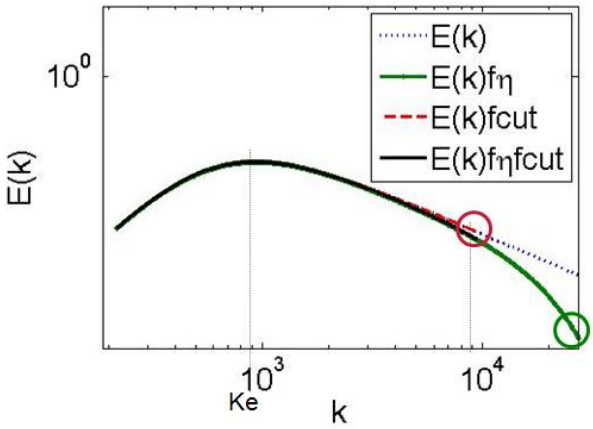


Figure 1: Normalized von Karman spectrum generated based on RANS solution and grid configuration.

order to clean the signal of undesired effects like summation of discretization errors, the velocity field is time-decorrelated by subtracting the time term of the equation (1) and generating new random values every time step. Autocorrelation is recovered afterwards by adding an asymmetric time filter [12] .

$$U'^m = aU'^{m-1} + bu'^m; \tag{5}$$

$$a = exp(-\frac{\Delta t}{\tau}) \tag{6}$$

$$b = \sqrt{1 - a^2} \tag{7}$$

Where $m$ is the time step number, $u'$ is the velocity fluctuation generated by the Synthetic Turbulence Generator, $U'$ is the time correlated velocity fluctuation and $\tau$ is the time scale which was calculated as defined by Adamian et al. [10] ($\tau = C_\tau \frac{l_e^{max}}{U}$). With the purpose of ensuring the robustness of the code, the synthetic fluctuations are introduced into the flow solution as a volume force acting in the momentum equation.

$$\underbrace{\frac{\partial}{\partial t}\int_\Omega \overrightarrow{W} d\Omega}_{\text{CONSERVATIVE VARIABLES}} + \underbrace{\oint_{\partial\Omega} (\overrightarrow{F_c} - \overrightarrow{F_v}) dS}_{\text{CONVECTIVE \& VISCOUS FLUXES}} = \underbrace{\frac{\partial}{\partial t}\int_\Omega \overrightarrow{Q} d\Omega}_{\text{SOURCE TERM}} \tag{8}$$

Where the source term is:

$$\overrightarrow{Q} = \begin{bmatrix} \rho U' \\ \rho V' \\ \rho W' \end{bmatrix} \tag{9}$$

# 3 Results

First of all a standalone version of Synthetic Turbulence Generator was implemented in order to assess the principal features of generated velocity field.
To do so, data was extracted from a flat plate boundary layer and used as input for the turbulence generator. Figure 2 shows a comparison between the components of the Reynolds stress tensors taken as reference and the one generated by the algorithm after 26800 iterations. It is seen that the model is able to reconstruct the stress tensors distribution.

In addition, output data was extracted at the location $z/\delta_0 = 0.86$ in order to evaluate the

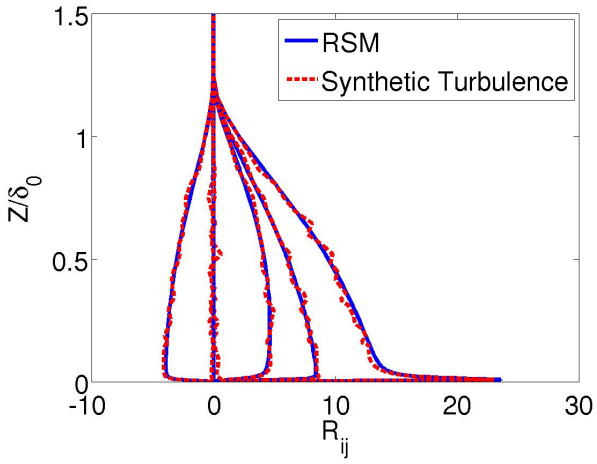


Figure 2: Comparison between the Reynolds stresses used as reference (RSM solution) and the ones generated by the synthetic turbulence generator

time and two-point correlations. The obtained distributions are shown in figure 3. From there, it can be deduced that this model provides fluctuations with time and spatial information of the turbulence.

As a first test case, the synthetic turbulence was inserted into a 2D flat plate boundary layer

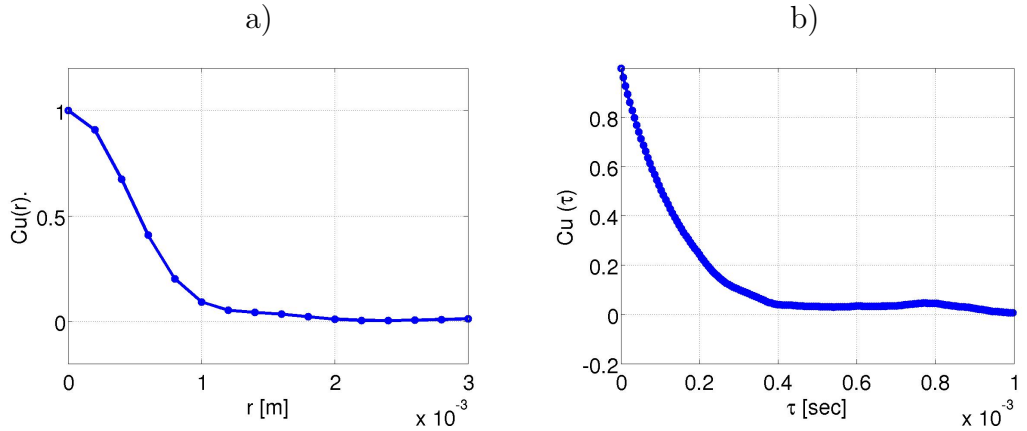


Figure 3: a) Two-point correlation coefficient at $z/\delta_0 = 0.86$, b) Time correlation coefficient at $z/\delta_0 = 0.86$

solved with the $\epsilon^h$-ADDES model and forced to switch from RANS to LES mode arbitrarily at position x = 0.65 m.

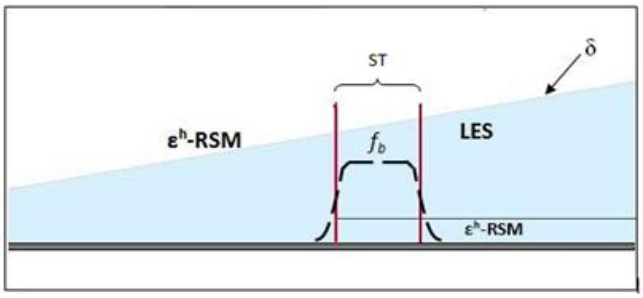


Figure 4: Sketch of the flat plate test case configuration

First, a flat plate with 1 m length was simulated. Simulations were performed at a Reynolds number of $R_e = 2.3.10^6$. The overall grid size was 270000 points. The grid spacing in the wall normal direction was designed to satisfy $y^+ = 1$ and in the stream direction $\Delta x^+ = 60$. The synthetic turbulence source term was activated in the range between x= 0.65 m and x=0.66 m. Figure 5 shows the Reynolds stress component $\overline{u'u'}$ for a pure $\epsilon^h$-ADDES simulation and the one with the synthetic turbulence generator activated. No important improvements are observable in this figure. Therefore, to have a better understanding of the changes brought onto the solution by the source term, 3 slices were extracted along the range where the synthetic turbulence was applied. In figure 6, reference stands for the Reynolds stresses distribution obtained from the RANS solution upstream of the RANS-LES interface and used as reference for the synthetic turbulence generator while ST denotes the standalone fluctuations as given by eq. [1]. Here, it can be observed that the field of velocity fluctuations generated by this method within the TAU-Code does regenerate the Reynolds stresses of the reference. Nevertheless, although the resolved turbulence appears to be increasing along these three locations, they never achieve a satisfactory magnitude.

To assess the evolution of these stresses along and beyond this range, another slice was

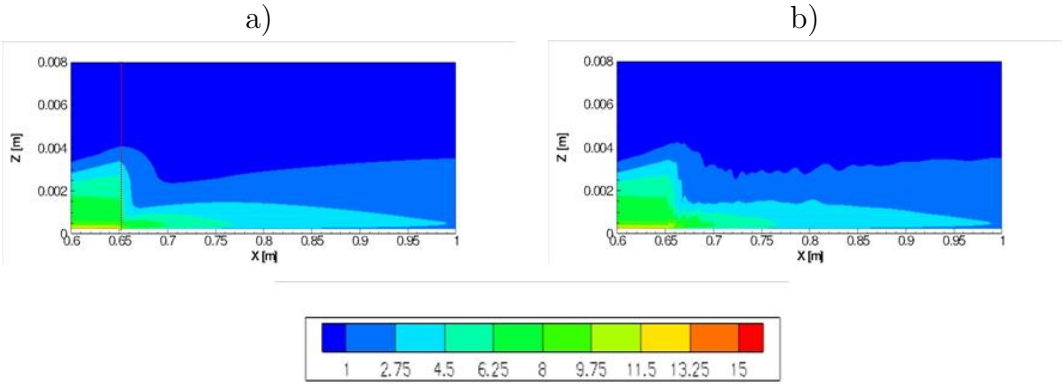


Figure 5: $\overline{u'u'}$ distribution a) Pure $\epsilon^h$-ADDES, b)$\epsilon^h$-ADDES plus Synthetic Turbulence Source Term

extracted but parallel to the wall at $z/\delta_0 = 0.21$. Figure 7, shows these distributions where it can be seen how the resolved turbulence actually increases along the whole range where the synthetic turbulence is applied but it quickly decreases until vanishing afterwards. In addition, it can be observed that the modelled turbulence by the sub-grid scale model is substantially larger than the solved one.

For these results, the first conclusion is that the high values of SGS (Sub-Grid Scale) stresses

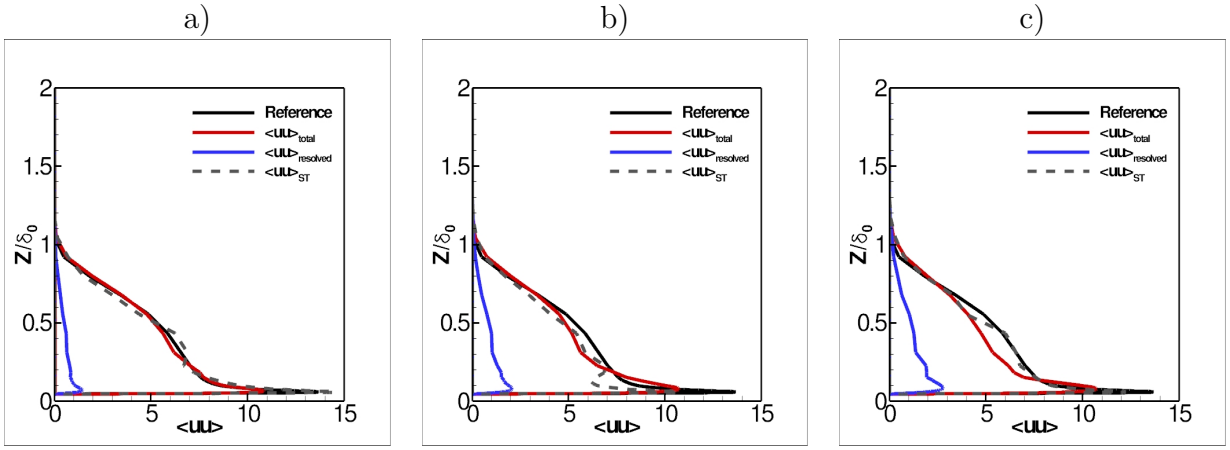


Figure 6: Distribution of $\overline{u'u'}$ at a) x=0.652 m , b) x=0.655 m and c) x=0.658 m.

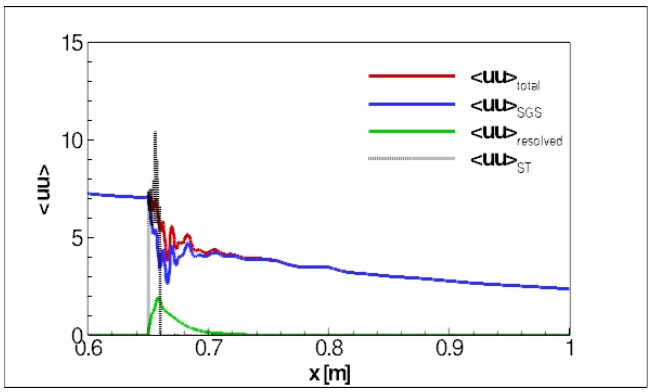


Figure 7: Reynolds stresses distribution at $z/\delta_0 = 0.21$

are dissipating the resolved ones. Hence, the same analysis was performed but with a new grid with a considerable smaller grid spacing. The new mesh had the same grid spacing in the wall normal direction but the spacing in the stream direction was reduced 3 times ($\Delta x^+ = 20$) in relation to the previous one($\Delta x^+ = 60$). For testing only the effects of reducing the sub-grid scale and in order to reduce the size of the grid, the length of the flat plate was reduced to 0.8 m. Figure 8 shows again the Reynolds stresses distributions at the positions x=0.652 m, x=0.655 m and x=0.658 m for this new configuration. Again, the Reynolds stresses of the synthetic turbulence field are in the order of the ones taken as reference. The same behaviour is observed for the resolved fluctuations whose Reynolds stresses increase slowly along the whole range in which the synthetic turbulence source term is activated but again they do not achieve satisfactory values. On the other hand, the total Reynolds stress which is the summation of the resolved and sub-grid scale ones decreases constantly along the range showing how the SGS scale Reynolds stress are reduced shortly after the transition.

Figure 9 shows the distributions along the stream direction at $z/\delta_0 = 0.21$. As for the coarser grid, the resolved stresses increase continuously along the range where the synthetic turbulence source term is activated and they vanish shortly afterwards. But now, the modelled turbulence was considerably reduced.

Comparing figure 9 with figure 7, it can be seen that applying the synthetic turbulence along the same range and under the same flow conditions, the resolved stress presents the same distribution for the coarser grid than for the finer one. In both cases, the resolved stresses

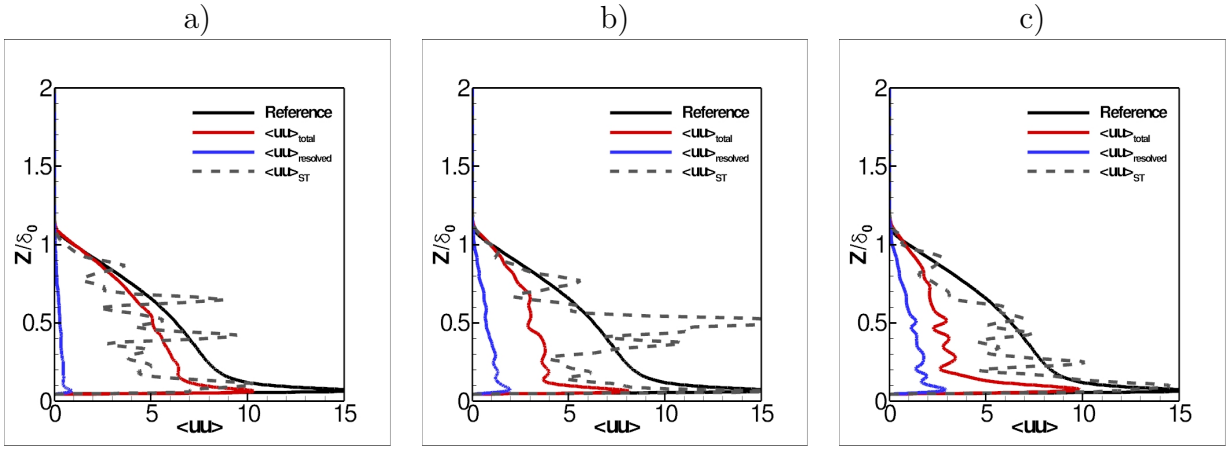


Figure 8: Distribution of $\overline{u'u'}$ at a) x=0.652 m , b) x=0.655 m and c) x=0.658 m.

achieve a maximum of about 2 $m^2/s^2$ and they completely vanish by x=0.7 m. This last observation leads to the conclusion that the resolved fluctuations don't depend significantly on the adopted SGS.

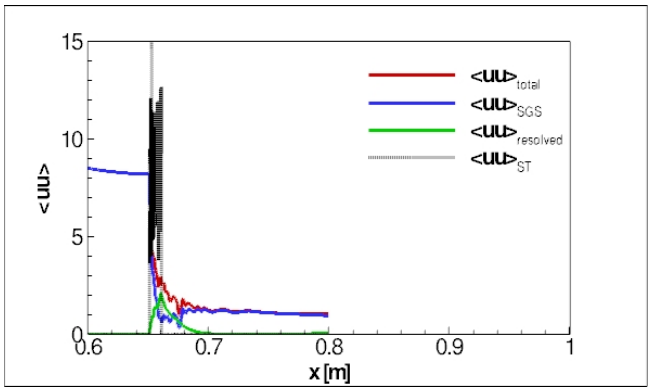


Figure 9: Reynolds stresses distribution at $z/\delta_0 = 0.21$

# 4 Conclusion

Although it is essential to have a fully 3D simulation in order to assess the real effectiveness of the implementation, the current results already allow drawing some important conclusions. The present synthetic turbulence generator is able to provide a field of velocity fluctuations which accurately reproduces the target Reynolds stresses distributions. In addition, it exhibits satisfactory time and two-point correlations. This physical behaviour is expected to be beneficial when applied to the 3D case in future steps.
First applications of the synthetic turbulence generator in 2D simulations of the DLR TAU-Code showed that the implementation is robust. Initial grid density studies indicate that the adopted sub-grid scale does not affect much the development of the resolved stresses. 3D simulations will show whether a reasonable level of resolved turbulence can be obtained with this approach.

# Acknowledgments

The members of the FOR 1066 research group gratefully acknowledge the support of the "Deutsche Forschungsgemeinschaft DFG" (German Research Foundation) which funded this research.

# References

[1] Spalart, P.R., Deck, S., Shur, M.L., Squires, K.D., Strelets, M., Travin, A., "A new version of detached-eddy simulation, resistant to ambiguous grid densities", Theoretical and Computational Fluid Dynamics, Vol. 20, No. 3, pp. 181-195, 2006.

[2] Probst, A., Radespiel, R., Wolf, C., Knopp, T., and Schwamborn, D., "A Comparison of Detached-Eddy Simulation and Reynolds-Stress Modelling Applied to the Flow over a Backward-Facing Step and an Airfoil at Stall", AIAA-2010-920, 48th AIAA Aerospace Sciences Meeting, Orlando, USA, 4-7 January 2010.

[3] Shur, M.L., Spalart, P. R., Strelets, M. and Travin, A.,"A hybrid RANS-LES approach with delayed-DES and wall-modelled LES capabilities", International Journal of Heat and Fluid Flow, Vol. 29, No. 6, pp. 1638-1649, December 2008.

[4] Knopp, T., Probst, A., "An Algebraic Sensor for the RANS-LES Switch in Delayed Detached-Eddy Simulation", 17th STAB/DGLR Symposium, Berlin, Nov 2010, submitted for publication in Notes on Numerical Fluid Mechanics and Multidisciplinary Design, Springer-Verlag, 2011.

[5] Jakirlić S. and Hanjalić K., "A new approach to modelling near-wall turbulence energy and stress dissipation", Journal of Fluid Mechanics, Vol. 459, 2002, pp. 139-166.

[6] Probst, A. and Radespiel, R., "Implementation and Extension of a Near-Wall Reynolds-Stress Model for Application to Aerodynamic Flows on Unstructured Meshes", AIAA-2008-770, 2008.

[7] Spalart, P. R., Allmaras, S. R. "A one-equation turbulence model for aerodynamic flows", La Recherche Aeorospatiale 1, 5-21, 1994.

[8] Laraufie R., Deck S., Sagaut P.,"A dynamic forcing method for unsteady turbulent inflow conditions", Journal of Computational Physics, Volume 230, Issue 23, p. 8647-8663, 2011.

[9] Sagaut P., Deck S., Terracol M., "Multiscale and multiresolution approaches in turbulence"., Imperial College Press., 2006.

[10] Adamian D., Travin A., "An Efficient Generator of Synthetic Turbulence at RANS-LES Interface in Embedded LES of Wall-Bounded and Free Shear Flows".,Computational Fluid Dynamics 2010, Russia, Springer , 2011, pp. 739-744.

[11] Batten P.,Chakravarthy S., Goldberg U., "Interfacing Statistical Turbulence Closures with Large-Eddy Simulation", AIAA Journal, vol. 42, issue 3, pp. 485-492, 2004.

[12] Davidson L., "Using isotropic synthetic fluctuations as inlet boundary conditions for unsteady simulations"., Advances and Applications in Fluid Mechanics, 2007.